

Effect of Heat Treatment on Precipitate Characteristics, Microstructure, and Mechanical Properties of Fe-12Cr-6Al Alloy Fabricated via Laser Powder Bed Fusion

Omer Cakmak^a, Hwasung Yeom^{a,b}, Jung-Wook Cho^{a,b*}

^aDivision of Advanced Nuclear Engineering, Pohang University of Science and Technology (POSTECH), Pohang, 37673, Republic of Korea

^bGraduate Institute of Ferrous & Eco Materials Technology, Pohang University of Science and Technology (POSTECH), Pohang, 37673, Republic of Korea

*Corresponding author: jungwook@postech.ac.kr

***Keywords: Heat treatment, Precipitates, Microstructure, Mechanical Properties, Laser-Powder Bed Fusion.**

1. Introduction

Iron-chromium-aluminum (FeCrAl) alloys exhibit exceptional resistance to oxidation at high temperatures, making them ideal for use in applications such as high-temperature heating elements and engine catalysts. Recently, these alloys have attracted attention in the nuclear field for their potential use as structural or accident-tolerant fuel cladding materials [1].

The production of FeCrAl alloys using Laser Powder Bed Fusion (LPBF), an additive manufacturing technique, offers several advantages. One key benefit is the ability to control the atmosphere during fabrication, enabling the in-situ formation of precipitates such as nitrides and oxides [2]. The uniform dispersion of these nano-sized precipitates within the matrix enhances mechanical properties, including hardness, strength, wear resistance, creep resistance, and corrosion resistance, allowing for the development of tailored materials for specific applications [3].

Understanding the impact of heat treatment on precipitate behavior, microstructural evolution, and mechanical properties is crucial for optimizing material performance to meet specific application requirements. Therefore, in this study, Fe12Cr6Al alloy was fabricated using LPBF in a nitrogen (N₂)-rich environment to facilitate the in-situ formation of nitride precipitates. The effects of heat treatment on precipitate characteristics, microstructure, and mechanical properties were systematically investigated.

2. Experimental Methods

The Fe-12Cr-6Al powder used in this study was sourced from MK Co. (South Korea) and produced via gas atomization, with a powder size distribution ranging from 15 to 45 μm . Specimens were fabricated using a Laser Powder Bed Fusion (L-PBF) system (Metalsys-250, WINFORSYS) under a nitrogen (N₂) atmosphere. The printing parameters were set to a laser power of 200 W, a scan speed of 400 mm/s, a layer thickness of 30 μm , and a hatch distance of 100 μm . The samples were printed with dimensions of 30 \times 10 \times 10 mm³.

The elemental composition of the as-built specimens, presented in Table 1, was determined using inductively coupled plasma-optical emission spectroscopy (ICP-OES, QSG-750, OBLF). To investigate the effects of heat treatment, three samples underwent annealing at 1200 °C for 1 hour in an air atmosphere, followed by air cooling after removal from the furnace. The morphology, size, and chemical composition of nitride and oxide precipitates in the as-built samples were characterized using a JEOL scanning electron microscope (SEM, JSM-7900F). Grain size distributions and average grain sizes were analyzed via electron backscatter diffraction (EBSD) with a step size of 0.5 μm over an analysis area of 562 mm². The EBSD data was further processed using HKL Channel-5 software.

To minimize surface roughness and eliminate defects, specimens were mechanically polished using silicon carbide (SiC) abrasive papers with grit sizes of 600, 800, and 1200. Subsequently, their tensile properties were evaluated at room temperature using a Universal Testing Machine (Instron-582, INSTRON) at a strain rate of 10⁻³ s⁻¹.

Table 1. Composition of FeCrAl alloy (wt. %).

Alloy	Fe	Cr	Al	O	N
FeCrAl	Bal.	12.77	6.84	0.015	0.0065

3. Results and discussion

3.1 Effect of heat treatment precipitates characteristics

SEM analysis was conducted on Fe12Cr6Al alloys both before and after heat treatment to examine the impact of heat treatment on the characteristics of in-situ formed nano-sized oxide and nitride precipitates. Figure 1a presents the SEM analysis of the as-built Fe12Cr6Al sample before heat treatment. As illustrated in Figure 1, prior to heat treatment, Al₂O₃ (Figure 1(a1), line graph) and AlN-O (Figure 1(a1), point identification) precipitates were identified within the Fe12Cr6Al alloy. According to the Ellingham diagram, the standard free energy of formation for Al₂O₃ is higher than that of

Fe₂O₃ and Cr₂O₃, indicating that oxygen (O) exhibits a stronger affinity for aluminum (Al) compared to iron (Fe) and chromium (Cr) [4]. Furthermore, during the solidification process in L-PBF, the rapid cooling rates may impede the diffusion of aluminum (Al), nitrogen (N), and oxygen (O), which were dissolved in the molten pool at elevated temperatures. Consequently, the formation of irregular AlN-O complex precipitates is likely to occur [5].

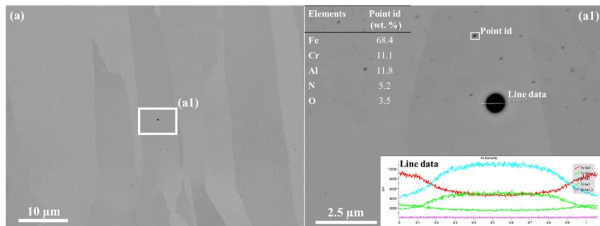


Fig.1. (a) Backscattered electron images and (a1) EDS line and point id results for precipitates analysis before heat treatment.

Analysis of the SEM images (Figure 2a) of the Fe12Cr6Al alloy after heat treatment at 1200°C for 1 hour indicates a substantial increase in precipitate density, with a homogeneous distribution throughout the matrix, including along grain boundaries. SEM-EDS mapping confirmed that these precipitates primarily consist of AlN (Figure 2(a1)). No other precipitate phases were identified in any of the examined samples. At high temperatures, such as 1200 °C in this study, the thermodynamic conditions of the system favor the formation of AlN over Al₂O₃. This preference arises due to the increased solubility of nitrogen in the matrix at elevated temperatures, facilitating its reaction with aluminum to form AlN, which is the more thermodynamically stable phase under these conditions [6][7].

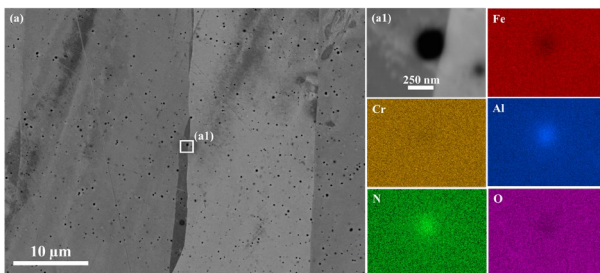


Fig.2. (a) Backscattered electron images and (a1) EDS maps results for precipitates analysis after heat treatment.

3.2 Effect of heat treatment microstructure

EBSD mapping was performed on samples with a cross-section parallel to the building direction both before (Figure 3a) and after heat treatment (Figure 3b). The analysis focused on characterizing the grain structure, including grain orientation, morphology, and size. Orientation maps obtained from the central region

of the Fe12Cr6Al sample, prior to (Figure 3a) and following (Figure 3b) heat treatment, indicate the presence of a columnar grain structure, with no significant changes observed after treatment. Heat treatment led to a slight increase in the average grain size from 71 μm (Figure 3(a1)) to 76 μm (Figure 3(b1)), while the overall grain size distribution remained largely unchanged.

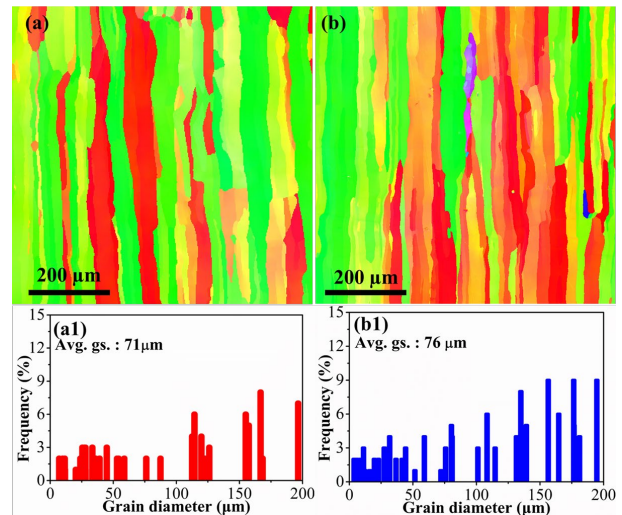


Fig.3. Scan direction IPF-X maps and grain size distribution analysis results of as build samples; (a, (a1)) before heat treatment and (b, (b1)) after heat treatment.

3.3 Effect of heat treatment mechanical properties

Figure 4 presents the mechanical test results for before and after heat-treatment for Fe12Cr6Al alloys. Heat treatment resulted in a decrease in yield strength (YS) by 110 MPa and ultimate tensile strength (UTS) by 78 MPa in the as-built sample, accompanied by a 3.5% increase in elongation (Table 1). The decrease in YS and UTS can be primarily attributed to grain growth during heat treatment, which diminishes the grain boundary strengthening effect, as well as a reduction in dislocation density induced by the heat treatment process. The observed improvement in ductility may be associated with this decrease in dislocation density, which reduces obstacles to plastic deformation [8]. The yield strength of the Fe-12Cr-6Al alloy evaluated in this study is comparatively lower than that of conventional zirconium-based coating materials. A reduced yield strength may necessitate the application of thicker coatings, which could, in turn, result in increased neutron absorption [9]. To address this limitation, our recent studies have demonstrated that the mechanical properties of the alloy can be significantly enhanced through the addition of alloying powders such as titanium (Ti) [2] and yttrium oxide (Y₂O₃) [3].

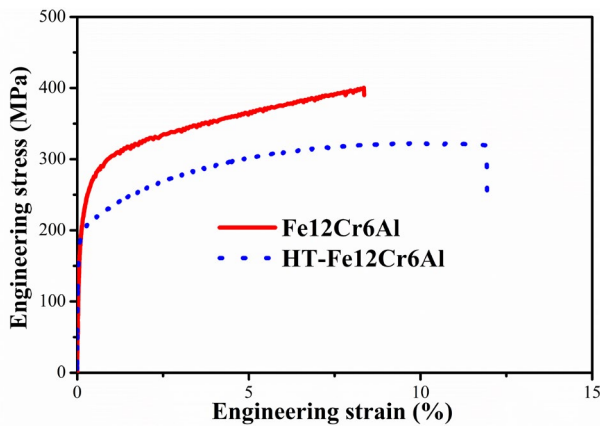


Fig.4. Stress-strain curves of Fe12Cr6Al alloys before and after heat treatment.

Table 1. Room-temperature mechanical properties of as-built samples prior to and following heat treatment.

Sample	Yield Strength (Mpa)	Ultimate tensile strength (Mpa)	Elongation (%)
Fe12Cr6Al	308 ± 10	403 ± 11	8 ± 2
HT-Fe12Cr6Al	198 ± 9	325 ± 10	3.5 ± 3

4. Conclusion

High-temperature heat treatment at 1200 °C-1 hour had a significant impact on the characteristics of nitride and oxide precipitates, as well as the microstructural and mechanical properties of Fe12Cr6Al alloys fabricated via LPBF in a nitrogen-rich environment. Nano-sized Al₂O₃ and AlN-O precipitates, which were present in the as-built samples, were no longer detected after heat treatment, leaving only AlN nano-precipitates. Grain size analysis indicated a slight increase in average grain size from 71 μm to 76 μm. Additionally, heat treatment led to a reduction in yield strength (YS) by 110 MPa and ultimate tensile strength (UTS) by 78 MPa in the as-built samples, while elongation increased by 3.5%.

REFERENCES

- [1] F. L. Article, "Journal of Alloys and Compounds New Insights on the Effects of Chemistry and Temperature on α' Precipitation During Aging of FeCrAl Alloys," *J. Nucl. Mater.*, vol. 605, no. November 2024, p. 155542, 2025, doi: 10.1016/j.jnucmat.2024.155542.
- [2] O. Cakmak, H. Yeom, and J. W. Cho, "In-situ synthesis of TiN and its effects on Fe-12Cr-6Al in laser powder bed fusion," *Addit. Manuf.*, vol. 84, no. November, pp. 6714–6721, 2024, doi: 10.1016/j.addma.2024.104148.
- [3] O. Cakmak, H. Yeom, and J. Cho, "In-situ synthesis of Ytria-based precipitates and their effects on Fe12Cr6Al in laser powder bed fusion," *J. Mater. Res. Technol.*, vol. 33, no. November, p. 6714-6721, 2024, doi: 10.1016/j.jmrt.2024.11.059.
- [4] S. Mirzababaei, M. Ghayoor, R. P. Doyle, and S. Pasebani, "In-situ manufacturing of ODS FeCrAlY alloy via laser powder bed fusion," *Mater. Lett.*, vol. 284, p. 129046, 2021, doi: 10.1016/j.matlet.2020.129046.
- [5] O. Cakmak, S. Lee, S. Gyu, D. Eo, H. Yeom, and J. W. Cho, "In-situ synthesis of nitrides and oxides through controlling reactive gas atmosphere during laser-powder bed fusion of Fe-12Cr-6Al," *Mater. Des.*, vol. 240, no. October 2023, p. 112862, 2024, doi: 10.1016/j.matdes.2024.112862.
- [6] C. C. Chen, C. Y. Chen, H. W. Yang, Y. K. Kuo, and J. S. Lin, "Phase Equilibrium in Carbothermal Reduction Al₂O₃ → AlN Studied by Thermodynamic Calculations," *Atlas J. Mater. Sci.*, vol. 1, no. 2, pp. 30–37, 2014, doi: 10.5147/ajms.2014.0172.
- [7] M. Boćkowski, B. Łuczniak, I. Grzegory, S. Krukowski, M. Wróblewski and S. Porowski, High-pressure direct synthesis of aluminium nitride, *J. Phys.: Condens. Matter* 14 (2002) 11237–11242.
- [8] Y. Zhang, H. Wang, H. Sun, and G. Chen, "Effects of annealing temperature on the microstructure, textures and tensile properties of cold-rolled Fe–13Cr–4Al alloys with different Nb contents," *Mater. Sci. Eng. A*, vol. 798, no. September, p. 140236, 2020, doi: 10.1016/j.msea.2020.140236.
- [9] G. R. Odette, M. J. Alinger, and B. D. Wirth, "Recent developments in irradiation-resistant steels," *Annu. Rev. Mater. Res.*, vol. 38, pp. 471–503, 2008, doi: 10.1146/annurev.matsci.38.060407.130315